



LAWRENCE
LIVERMORE
NATIONAL
LABORATORY

Advances in Quantum Monte Carlo

N. Tubman, J. L. Dubois, B. Alder

August 17, 2011

Advances in Quantum Monte Carlo

Disclaimer

This document was prepared as an account of work sponsored by an agency of the United States government. Neither the United States government nor Lawrence Livermore National Security, LLC, nor any of their employees makes any warranty, expressed or implied, or assumes any legal liability or responsibility for the accuracy, completeness, or usefulness of any information, apparatus, product, or process disclosed, or represents that its use would not infringe privately owned rights. Reference herein to any specific commercial product, process, or service by trade name, trademark, manufacturer, or otherwise does not necessarily constitute or imply its endorsement, recommendation, or favoring by the United States government or Lawrence Livermore National Security, LLC. The views and opinions of authors expressed herein do not necessarily state or reflect those of the United States government or Lawrence Livermore National Security, LLC, and shall not be used for advertising or product endorsement purposes.

RESERVE THIS SPACE

Recent results in the exact treatment of fermions at zero and finite temperature

NORM M. TUBMAN^{1,2}

JONATHAN L DuBOIS¹

BERNI J. ALDER¹

¹Lawrence Livermore National Laboratory, Livermore, CA

²Department of Physics, University of Illinois, Urbana-Champaign, Illinois

We present release-node quantum Monte Carlo simulations of the first row diatomic molecules and assess how accurately their ground state energies can be obtained with current computational resources. An explicit analysis of the fermion-boson energy difference shows a strong dependence on the nuclear charge, Z , which in turn determines the growth of the variance of the release-node energy. We show that efficiency gains from maximum entropy analysis are modest and that extrapolation to the ground state is tractable only for the low Z elements. For finite temperatures we discuss what can be gleaned from the structure of permutation space for interacting Fermi systems. We then demonstrate improved efficiency in the exact path integral Monte Carlo treatment of liquid ^3He by using importance sampling to deemphasize the contribution of long permutation cycles to the partition function.

RESERVE THIS SPACE

Exact methods at T=0

The fundamental goal in the field of *ab-initio* simulations is to perform electronic calculations to high accuracy or, even better, exactly. To simulate exact methods an exponentially increasing amount of resources seems to be needed, and thus in practice system sizes are often severely restricted. For example, two well-known methods which are in principle exact are configuration interaction and density functional theory. Here, the exponential computational complexity is manifest in the formulation of configuration interaction [1], and is less obvious in DFT where it arises as a problem in generating exact functionals [2]. As a result, practical uses of these algorithms do not yield exact results.

Release-node quantum Monte Carlo (RN-QMC) is a simulation method that allows the eigenstates of a Hamiltonian to be sampled without any systematic bias. The method is computationally expensive, however, and there are significant limitations to what can feasibly be simulated. For quantum Monte Carlo (QMC) calculations this has led to the development of the popular but approximate fixed-node diffusion Monte Carlo (FN-DMC). Despite the possibility of improved accuracy, RN-QMC has only been used in a relatively limited number of simulations. Nonetheless there have been some notable applications and algorithmic developments.

One such application in which RN-QMC has been successful is the electron gas [3] where hundreds of electrons have been simulated without convergence problems. Convergence of a RN-QMC calculation is dependent on two decay parameters given by $\tau_1 = E_0^F - E_0^B$ which determines the imaginary-time growth of the variance, and $\tau_2 = E_1^F - E_0^B$ which determines the slowest imaginary-time decay of the excited antisymmetric components relative to the fermion ground state. The energies E_0^F , E_0^B , and E_1^F are the fermion ground state, the boson ground state and the first excited fermion state, respectively. Hamiltonians in which the fermion-boson energy gap is small are well suited for RN-QMC simulations, and the free electron gas is one such Hamiltonian. Nuclear charge centers change the situation significantly such that relatively small atoms have large fermion-boson energy gaps. The largest molecular RN-QMC calculations to date have been performed on systems of around 10 electrons. However, even in these cases, convergence is not always attained. In the first RN-QMC calculations of molecules [4] several systems were simulated including H_2O and Li_2 molecules. Later RN-QMC calculations included systems such as HF [5], LiH [6], and H_2+H [7] in which RN-QMC was able to reach higher accuracies as a result of algorithmic modifications and increased computational resources. Our goal is to consider the range of Hamiltonians that can be practically simulated with RN-QMC with current computational power and modern algorithms. In particular we have applied the method to the simulation of the first row dimers with an accuracy goal of 10^{-3} [a.u.].

Released node Quantum Monte Carlo

We can understand how RN-QMC achieves exact results by considering the eigenfunction expansion of the imaginary time propagator

$$e^{-t(H-E_T)} = \sum_i e^{-t(E_i-E_T)} |\Phi_i\rangle \langle \Phi_i|. \quad (1)$$

For $E_T = E_0$ the asymptotic, $t \rightarrow \infty$, limit of this operator gives the ground state of the Hamiltonian. Technically a RN-QMC calculation is only converged in this limit, however in practice we consider a RN-QMC calculation converged when the slope of the release-node energy estimator is zero to within the statistical error. This occurs when the standard error of our energy estimate at a given imaginary time is larger than the final energy difference to be decayed in the asymptotic limit. As imaginary time increases with repeated application of the propagator in equation (1), all excited states decay relative to the ground state. If a trial function, $\Psi_T(X)$, is used for importance sampling, the asymptotic distribution will be:

$$\lim_{t \rightarrow \infty} \sum_i e^{-t(E_i-E_T)} |\Phi_i\rangle \langle \Phi_i | \psi_T \rangle \approx e^{-t(E_0-E_T)} |\Phi_0\rangle \langle \Phi_0 | \psi_T \rangle. \quad (2)$$

For a standard molecular Hamiltonian the ground state wave function is a boson state and the fermion ground state is an excited state of the Hamiltonian. Like all other excited states, it decays exponentially relative to the ground state with application of the imaginary-time propagator. In certain cases we can accurately measure the fermion ground state as it decays in imaginary time. To determine the fermion ground state we can make a projection onto the antisymmetric subspace during this decay process.

The antisymmetric projection is problematic for many Hamiltonians. The release-node method is an example of a transient algorithm since the fermion ground state is decaying exponentially in the limit of large imaginary time. The release process is initiated with the introduction of a nodeless guide wave function, $\Psi_G(X)$, such that the walkers will equilibrate to the boson ground state. During this process an antisymmetric trial wave function is used to project out the antisymmetric signal. This causes a sign problem that manifests in the simulation as exponentially growing noise in the release-node energy estimate.

The release-node energy can be calculated in a similar form to the FN-DMC

$$E_0^{RN} = \frac{\sum_i W_i R(\mathbf{X}_i) E_L^T(\mathbf{X}_i)}{\sum_i W_i R(\mathbf{X}_i)}. \quad (3)$$

This estimator involves the sum of positive and negative terms, given by the sign of the trial wave-function as seen in the term $R = \Psi_T(X)/\Psi_G(X)$, which is the reweighting factor for the guiding wave function. The weight of the i th walker is calculated as

$$W = \prod_j e^{-t/2(E_L^G(\mathbf{R}_j)+E_L^G(\mathbf{R}_{j+1}))} \quad (4)$$

where the product is over all previous positions the walker has traversed. The terms E_L^T and E_L^G are the local energies of the trial wave-function and the guiding function respectively. The form of the local energy is given by $E_L^{G,T} = \Psi_{G,T}^{-1} H \Psi_{G,T}$. It can be shown that the variance of the transient energy E_0^{RN} is proportional to a growing exponential with imaginary time [8,9]:

$$\sigma^2(E_0^{RN}) \propto e^{2t(E_0^F - E_0^B)}. \quad (5)$$

The release-node estimate for the energy will start decaying from the FN-DMC energy, and eventually it will become flat, while the variance will continue to grow as given in equation (4). The convergence rate from the FN-DMC energy to the fermion ground state energy is different for each of the component eigenstates present in the fixed-node wave function. Ideally one would like a fast decay of the fermion excited states, and a slow increase of the variance, i.e. $(E_1^F - E_0^F) \gg (E_0^F - E_0^B)$. In this ideal situation one can hope to sample E_0^F at a large imaginary time with relatively small variance.

Fermion-boson gaps

The actual cost of a RN-QMC calculation is somewhat complicated by the introduction of a trial wave function. A good trial wave function can significantly decrease the contamination from the excited states, improving the convergence of the release algorithm. In the limit that the trial wave function has the correct nodal structure, FN-QMC gives the ground state energy and RN-QMC will be flat as a function of imaginary time. Therefore generating high quality RN-QMC results involves a balance of computing the best wave function possible and running release-node for as much imaginary time as possible. Once a trial wave function is optimized and put into a release-node calculation it is the growth of the variance as a function of imaginary time that prevents a calculation from converging. It can be seen from equation (5) that this is independent of the trial wave function.

With this behavior of the variance it is important that the excited states decay away before the simulation is overwhelmed with noise. For the first-row dimers, excluding Li_2 , we have estimated the amount of time needed to converge

our starting FN-DMC starting wave functions¹¹ to an accuracy greater than 10^{-3} [a.u.] will be greater than 1 [a.u.]⁻¹. A more accurate estimate of the convergence times is dependent on the magnitude of the excited state components of the FN-DMC wave function. Since the rate of growth of the variance is determined by the fermion-boson energy gap, it is important to understand how a Hamiltonian influences this energy gap. We recently made some calculations of the fermion-boson energy differences for the first-row dimers shown in Table I. The fermion energies are calculated from FN-DMC and the boson energies are calculated with unrestricted Diffusion Monte Carlo (DMC) using nodeless guiding wave functions. The boson energies are measured without any systematic errors, while the fermion energies have systematic errors corresponding to errors in the nodal surfaces. These systematic errors are estimated to be much smaller than 1 [a.u.] and are much smaller than the scale of the fermion-boson energy differences. The fermion-boson energy differences cover a range of about two orders of magnitude across the first-row dimers. As previously mentioned, we would like to simulate at least 1 [a.u.]⁻¹ of imaginary time during the release process, however the size of these fermion-boson gaps imply that the variance will grow to intractable sizes for most of the first row dimers well before 1 [a.u.]⁻¹ of simulation time.

Table I. Fermion Boson energy gaps for the second row dimers. Boson ground states are measured without any systematic errors with DMC, while the fermion energies are taken as the estimated exact values from reference [11]. All energies are in Hartree.

TABLE I.	
System	$E_0^F - E_0^B$
Li ₂	2.4
Be ₂	9.2
B ₂	22.9
C ₂	45.7
N ₂	79.9
O ₂	109.5
F ₂	192.4

In a recent RN-QMC study of the first row dimers [10], for a given set of trial wave functions [11], we were able to achieve an accuracy of 10^{-4} [a.u.] for Li₂, however we were not able to achieved our desired accuracy of 10^{-3} for any of the other first row dimers.

Improving Release Node

While performing RN-QMC on better wave functions will always lead to better results, there are several methods have been proposed to reduce the computational cost of RN-QMC – some of which have the promise of removing the exponential scaling of the algorithm. In this section we consider a few of the more promising techniques which are imaginary time projections and walker cancellation.

Projection techniques are based on sampling quantities during the release process, other than the RN-QMC energy estimator, to project out the ground state energy. It is known that some of these quantities, which are called imaginary time correlators, have simple imaginary-time dependence of the eigenvalue spectrum. After generating samples of a correlator of interest, we can fit the data and extract out the ground-state energy. The benefit of such an approach is that a highly accurate estimate of the ground-state energy might be possible with a limited amount of imaginary-time data. The idea of fitting imaginary time data is a general concept that has been applied very broadly in computational physics and other fields [12]. As far as applications of this for RN-QMC calculations, only the LiH molecule and various model Hamiltonians have tested these ideas [6,13,14].

Projecting out the ground state energy with this imaginary time data is equivalent to performing an inverse Laplace transform. The inverse Laplace transform is known to be sensitive to noisy data and we used a Maximum Entropy technique in our calculations to reduce our sensitivity to noise. We showed significantly better results than our standard release-node calculations [10], as we were able to generate ground state energies for Li_2 , Be_2 , and B_2 with this approach. However, due to the nature of the inverse Laplace transform, our results were too noisy to properly project out ground state energies for the rest of the first row dimers. Our analysis suggests that these projection techniques that rely on inverse Laplace techniques, although more efficient than standard RN-QMC, do not get around the exponential scaling of the problem and practically can not be applied to larger systems.

Cancellation techniques provide an alternative route to improving on the efficiency of the RN-QMC method. It has been demonstrated that, by allowing walkers of opposite sign to annihilate each other, cancellation can slow down the growth rate of the error. To date, this approach has been applied to a number of problems with varying success [15]. In addition, cancellation has also been applied in molecular calculations for linear H-H-H and H_2 [16]. A recent study demonstrating promising behavior of the technique in high dimensional systems is worth noting [17].

Exact methods at finite temperature

Path integral quantum Monte Carlo (PIMC) methods have provided significant insights into the low temperature properties of bosonic quantum liquids and solids (see e.g. [18]). And while the approach can, in principle, be applied to simulate the full many-body partition function for fermions as well, a sign problem occurs for temperatures below the $T \rightarrow \infty$ limit. As a result, enforcement of Fermi symmetry for all but the smallest finite temperature systems has in practice required the invocation of an uncontrolled approximation in the form of a restriction on the phase space of the path integral in order to prevent sign changes [19,20]. In this section we discuss what is known about the nature of the sign problem at finite T and describe an approach for reducing its effects.

PIMC methods work by sampling a product of approximate high temperature (short imaginary time) density matrices (Green functions) $\exp[-\beta\hat{H}] = \exp[-(\beta/M)\hat{H}]^M$ just as in ground state QMC methods like DMC. The differences between the methods arise mainly from the fact that sampling of a fixed finite temperature ensemble imposes a periodicity on the permuted coordinates in β , i.e.

$$\rho(\mathbf{R}; \beta) \propto \sum_{\mathcal{P}} (-1)^{\mathcal{P}} \langle \mathbf{R} | e^{-\frac{\beta}{M}\mathcal{H}} | \mathbf{R}_1 \rangle \langle \mathbf{R}_1 | e^{-\frac{\beta}{M}\mathcal{H}} | \mathbf{R}_2 \rangle \dots \langle \mathbf{R}_{M-1} | e^{-\frac{\beta}{M}\mathcal{H}} | \mathcal{P}[\mathbf{R}] \rangle. \quad (6)$$

where the sum is over the symmetric group and $\mathcal{P}[\mathbf{R}]$ represents a permutation of the many-body coordinate \mathbf{R} . In ground state methods this periodicity formally only exists at $\mathbf{R}_{\beta \rightarrow \infty}$, and antisymmetry may be imposed by an explicit projection at each time slice as described above. In canonical PIMC, however, the β periodicity of $\mathcal{P}[\mathbf{R}]$ requires that permutations be sampled explicitly and so configuration space typically consists of complete paths $Y = \{\mathbf{R}, \mathbf{R}_1, \mathbf{R}_2, \dots, \mathbf{R}_{M-1}\}$ where \mathbf{R}_{M-1} must be connected to $\mathcal{P}[\mathbf{R}]$ by the high temperature density matrix $\exp[-(\beta/M)\hat{H}]$. The sum over permutations in e.q. (6) is clearly the source of the sign problem in finite temperature PIMC. However, the explicit representation of permutations as linked polymers and in particular the connection between the length of a permutation (i.e. the number of particles participating in a single closed loop) and the kinetic energy leads to some interesting and useful observations about the structure of permutation space and, consequently, the finite T sign problem as well.

The structure of permutation space

While there are $N!$ possible permutations of N particles, the symmetry group can be further organized into subsets of topologically equivalent diagrams [21,22].

Figure 1 shows representative members from the five equivalence classes of the Symmetric group for four particles, S_4 . It is easy to see that if each of these classes was equally probable, the sum over all of them would indeed be zero and, as a result, the antisymmetric ‘signal’ embedded in the partition function would disappear. At any finite temperature, however, each equivalent permutation sector will have a different mean energy and therefore a different probability and the total contribution to the antisymmetrized partition function will be nonzero. For this reason one might be so bold as to say that at finite temperature there is not a sign problem but merely a “sign annoyance.”

In practice, while the number of equivalence classes grows roughly as $N^{7/2}$ [23] – much more slowly than the $N!$ number of enumerated permutations -- the contribution to the partition function of neighboring high order sectors (i.e. those consisting of long permutation cycles) becomes nearly identical at even moderately low temperatures. As a result, if the partition function is sampled directly, most of the simulation time will be spent generating configurations that will ultimately cancel each other out.

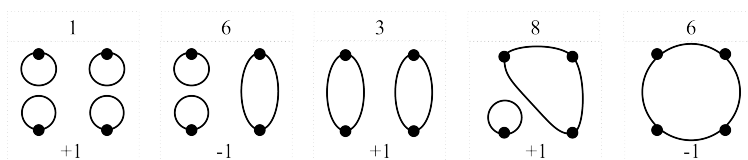


Figure 1: Diagrammatic representation of the equivalence classes of the symmetric group for 4 particles, S_4 , the number of elements in each class (top), and the sign of the contribution of members of each class to the partition function (bottom).

In addition to recognizing the relative importance of low order permutation sectors, it is instructive to examine the connection between the order of a permutation sector and the mean kinetic energy. Intuitively, long permutations impose a weaker constraint on the paths of participating particles since a path consisting of v particles only need return to its starting point after imaginary time $v\beta$. As a consequence, in an isotropic system longer permutation cycles will, on average, have lower kinetic energy than short ones. For the noninteracting gas this connection is especially clear as the contribution to the partition function from v permuting particles is equivalent to the single particle partition function at a lower temperature $Z_1(v/T)$. As a result, the mean energy of paths in each permutation sector is monotonically decreasing with the order of the sector. For fixed particle number, the virial theorem tells us that this trend must hold for systems with pairwise interactions as well.

Motivated by these observations we have recently explored the possibility of improving the efficiency of PIMC simulations applied to Fermi systems by using importance sampling to limit the time spent evaluating nearly degenerate

permutation classes. The approach is relatively straightforward. Starting with the recently developed continuous-space worm algorithm [24,25] to efficiently sample permutation space, we employ standard importance sampling techniques to modify the probability of moves that change the permutation sector. Sampling of long permutation cycles is penalized by reducing the probability of attempting moves that will extend the length of a permutation while the acceptance probability of such moves is increased to maintain detailed balance. The net result is that low order permutation sectors (those with only a few short permutation cycles) are sampled a great deal and high orders very rarely. In addition, the energy of each equivalence class is binned separately so that the final expectation value for the energy is taken by summing over the mean energy in each class multiplied by the probability of being in the class. Finally, using the knowledge that both the mean energy per sector E_g and the

$$\langle E \rangle = \sum_g Sgn[g](\bar{E}_g + \sigma_E)(\bar{n}_g + \sigma_n) \approx \sum_g Sgn[g]\tilde{E}[g]\tilde{n}[g] + \tilde{\sigma}_E\tilde{\sigma}_n. \quad (7)$$

probability of occupying each sector n_g are monotonically decreasing functions, an improved estimate of the mean energy is obtained by fitting E_g and n_g to smoothly decaying functions $E[g]$ and $n[g]$. The $\sigma_{E,n}$ in eq (7) represent the statistical error in the energy and probability density respectively in each sector while $\tilde{\sigma}_{E,n}$ are the error resulting from fitting energies and probability density over all sectors using a model. This step can in principle introduce a systematic error but it is not strictly necessary. We also note that since sampling is performed in the grand canonical ensemble, the chemical potential, μ , is a parameter. In the results for ^3He below we have fixed μ so as to match the known experimental density. A more detailed account of this “exchange truncated grand canonical PIMC method” will be presented elsewhere [26].

Results of a simulation of $N=66$ ^3He particles using the Aziz potential [27]

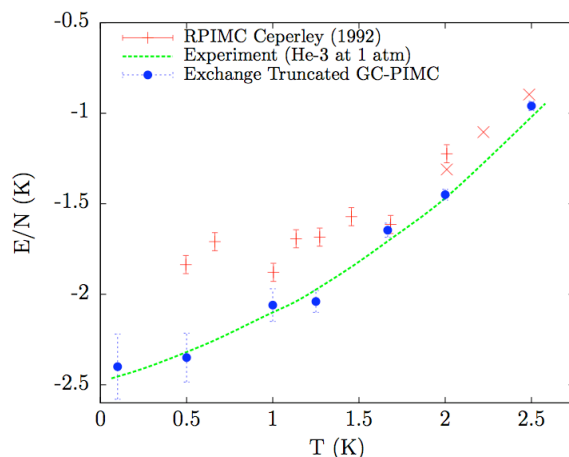


Figure 2 Results of Exchange Truncated Grand Canonical PIMC applied to liquid ^3He . Our results (solid circles) agree well with experimental data (dashed line) down to temperatures well below the ^3He Fermi temperature. The improvement over the approximate restricted path integral method (+ symbols), a 25% difference in energy per particle at 0.5 K, is evident.

and the approach outlined above are shown in Figure 2. Our results for the temperature dependence of the energy are in very good agreement with experiment. In contrast, it can be seen that the restricted path approach [19] suffers from a comparatively large systematic error. Also of note is that we are able to obtain results well below the Fermi temperature of ^3He despite the fact that, in principle, exact treatment of the partition function requires sampling of $66! \sim 10^{92}$ permutations and ~ 6000 equivalent permutation groups.

Conclusion

We have applied the RN-QMC method to the first row dimmers in an attempt to quantify the level of accuracy obtainable for all-electron chemical systems with this approach using current resources. Our results indicate that release node projections can be converged for up to ~ 10 electrons with an accuracy of at least 10^{-3} . We find that while maximum entropy analysis of the imaginary time decay significantly improves estimates of the ground state energy, it does directly not solve the problem of the poor scaling of the computational cost of RN-QMC for a fixed error bar with Z . For finite temperatures we reviewed some of what is known about the nature of the sign problem and presented results of a new scheme for taking advantage of the structure in permutation space by neglecting contributions from long permutation cycles. An open area for future research in this area involves the generalization of our approach to inhomogeneous systems.

References

-
- ¹ A. Szabo and N. Ostlund. *Modern Quantum Chemistry*. Dover, 1982.
 - ² N. Schuch and F. Verstraete. *Nat. Phys.*, **5**:732, 2009.
 - ³ D. M. Ceperley and B. J. Alder. *Phys. Rev. Lett.*, **45**:566, (1980).
 - ⁴ D. M. Ceperley and B. J. Alder. *J. Chem. Phys.*, **81**:5833, (1984).
 - ⁵ A. Lüchow and J. B. Anderson. *J. Chem. Phys.*, **105**:4636, (1996).
 - ⁶ M. Caffarel and D. M. Ceperley. *J. Chem. Phys.*, **97**:8415, (1992).
 - ⁷ D. L. Diedrich and J. B. Anderson. *J. Chem. Phys.*, **100**:8089, (1994).
 - ⁸ R. Assaraf, M. Caffarel, and A. Khelif. **40**:1181, (2007).
 - ⁹ I. Morgenstern, *Z. Phys. B* **77**, 267 (1989).
 - ¹⁰ N. M. Tubman, J. L DuBois, R. Q. Hood, B. J. Alder, *J. Chem. Phys.*, **135**:184109, (2011).
 - ¹¹ C. Filippi and C. J. Umrigar. *J. Chem. Phys.*, **105**:213, (1996).
 - ¹² M. Jarrell and J.E. Gubernatis. *Phys. Rep.*, **269**:133, (1996).
 - ¹³ M. Caffarel, M. Gadea, and D. M. Ceperley. *Europhys. Lett.*, **16**:249, (1991).

-
- ¹⁴ D. Blume, M. Lewerenz, P. Niyaz. and K. B. Whaley, Phys. Rev. E, **55**:3664, (1997).
- ¹⁵ D. M. Arnow, M. H. Kalos. J. Chem. Phys., *77*:5562, (1982), M. H. Kalos. Phys. Rev. E, **53**:5420, (1996), S. Zhang and M. H. Kalos. Phys. Rev. Lett., **67**:3074, (1991), M. H. Kalos and Francesco Pederiva. Phys. Rev. Lett., **85**:3547, (2000).
- ¹⁶ J. B. Anderson, C. A. Traynor, and B. M. Boghosian. J. Chem. Phys., **95**:7418, (1991).
- ¹⁷ F. Arias de Saavedra, M. H. Kalos, and F. Pederiva. Mol. Phys., DOI: 10.1080/00268976.2011.604647, in press.
- ¹⁸ D. M. Ceperley. Rev. Mod. Phys., **67**:279 (1995)
- ¹⁹ D. M. Ceperley. Phys. Rev. Lett., **69**:331 (1992).
- ²⁰ D. M. Ceperley. in *Monte Carlo and Molecular Dynamics of Condensed Matter Systems*, Ed. K. Binder and G. Ciccotti, Editrice Compositori, Bologna, Italy, (1996)
- ²¹ R. P. Feynman, Statistical Mechanics (Benjamin, New York, 1972).
- ²² J. P. Elliot and P. G. Dawber, Symmetry in Physics (Macmillan, London, 1979).
- ²³ A. P. Lyubartsev and P. N. Vorontsov-Velyaminov., Phys. Rev. A, **48**:4075 (1993).
- ²⁴ M. Boninsegni, N. V. Prokofev and B. V. Svistunov. Phys. Rev. Lett., **96**:070601 (2006).
- ²⁵ M. Boninsegni, N. V. Prokofev and B. V. Svistunov. Phys. Rev. E, **74**:036701 (2006).
- ²⁶ J. L DuBois and B. J. Alder. *In preparation*
- ²⁷ R. A. Aziz, V. P. S. Nain, J. S. Carley, W. L. Taylor, and G. T. McConville, J. Chem. Phys., **70**:4330 (1979).

Prepared by LLNL under Contract DE-AC52-07NA27344.